Unsteady aerodynamics over surface of a chambered airfoil at stall angle and low Reynolds number

Gamze Genç[1,*], *Kemal* Koca[1], *Mustafa Serdar* Genç[1]

[1]Wind Engineering and Aerodynamic Research Center, Department of Energy Systems Engineering, Erciyes University, Kayseri, TURKEY

Abstract. The proposal of this paper is clear to reveal and understand the unsteady flow characteristics over the surface of chambered airfoil operating especially at low Reynolds numbers by detecting boundary layer separation and laminar separation bubble (LSB). Experiments including smoke-wire technique for flow visualization, velocity measurement via hot-wire sensor and quasi-wall shear stress measurement by means of the hot-film sensor have been performed over the suction surface of NACA 4412 airfoil at Reynolds number of $5x10^4$ and angle of attack of 14°. Experiments indicate that the airfoil at a stall angle exhibits the bistable characteristics over the suction surface because of the unsteady bubble bursting at low Reynolds numbers. That is, either laminar flow separates from the leading-edge of the airfoil owing to a dominant adverse pressure gradient (APG) or it does not separate along downstream. It is also noted that unsteady boundary layer formation may affect the flow characteristics by changing airfoil's stability appreciably, causing the periodic fluctuations with the occurring bubble bursting and the leading edge and trailing edge vortex merging. This may conclude undesirable problems such as noise, vibration and flutter for the flight vehicles and wind turbines.

1 Introduction

Understanding of flow characteristics around airfoils is crucial in engineering systems including micro air vehicles, small-scale wind turbines and unmanned aerial vehicles operating at low Reynolds numbers regime ($1x10^4<Re<5x10^5$) [1], because these directly influence the aerodynamic performance of wind turbines and aircrafts' energy consumption. Therefore, they have been investigated in detail recently. Since the high drag and low lift generated in these flow regimes, the aerodynamic performance of the aforementioned engineering applications has been frequently gained attentions by researchers [2].

The essential impediment for aerial vehicles operating at low Reynolds numbers is laminar boundary layer separation [3]. The flow behaviour at low Reynolds numbers regimes is different from flow at higher Reynolds numbers because APG plays a dominant role and opposes the incoming flow, causing the boundary layer to separate from the surface [4]. After a while, separated flow in the transition region may reattach to the surface by gaining momentum, leading to the occurrence of a laminar separation bubble (LSB) over the surface. The laminar separated shear layer at low Reynolds numbers and higher angles of attack are highly unstable. Therefore, aerodynamic researchers have made a contribution to the understanding of flow development and unstable flow phenomena in the separated region and, especially, transition region [5-7]. Mechanism of boundary layer separation and flow transition in a separated shear layer over a NACA0012 airfoil at $Rec=5x10^4$ was numerically investigated with Direct Numerical Simulation (DNS) by Rodriguez et al. [8]. They found that airfoil exhibited a composition of training / leading edges stall, bringing about massive flow separation. Simoni et al. [9] carried out an experimental study to investigate laminar boundary layer separation, shear layer transition and reattachment phenomena at $Re=7x10^4$ and $Re=1x10^5$. Their conclusion revealed that the essential mechanism of transition is the inviscid Kelvin-Helmholtz instability. They also concluded that lower frequency oscillations must be amplified and reach satiation for emerging of transition. LSB on a NACA0012 airfoil at $Re_c=5x10^4$ was investigated by Jones et al. [10]. They also discussed that the effect of volume forcing is important for the promotion of transition to turbulence. Koca et al.

* Corresponding author: gamzegenc@erciyes.edu.tr

[5], Genç et al. [11-12], Karasu et al. [13], Ducoin et al. [14], Lambert and Yarusevych [15] investigated the vortex dynamics in LSB (leading edge vortex) and wake region of airfoils (trailing edge vortex) with a chance of angle of attack and Reynolds number. Their results showed that the size of LSB decreased and vortex shedding characteristics changed when the angle of attack increased, causing the shedding frequency to increase and the streamwise wavelength to reduce.

The purpose of this letter is to reveal the unsteady flow characteristics, LSB and transition to turbulence formation on NACA 4412 airfoil with experiments including velocity measurement, time-dependent flow visualization and quasi-wall shear stress measurement by means of hot-wire, smoke-wire and hot-film sensor, respectively. All experiments have been conducted at Rec=5x10^4 and angle of attack of (α) of 14°.

2 Experimental Rigs

The experiments have been performed in a low-speed wind tunnel having a square test section of 500mm x 500mm as shown in Figure 1. The detailed information about wind tunnel can be found in the authors' previous studies [5, 16, 17]. NACA 4412 airfoil as the experimental test model has been fabricated by means of 3D printer [11].Two transparent plexiglass end-plates have been attached at each tip of the airfoil to be protected the effect of tip-vortices while allowing the researchers to observe flow patterns over surface easily.

Fig. 1. Experimental set-up.

2.1 Flow visualization system

Regarding smoke-wire and hot-wire experiments, a sketch has been ensured as illustrated in Figure 2. The smoke-wire consists of the electrically resistive heating to burn oil, a wire with 0.03 mm diameter, three halogen lamps, a compact camera and oil. The wire has been vertically positioned at a distance of 1c (chord length) in front of leading-edge of the airfoil. The electrically resistive heating has been used to heat when oil has been manually dropped at the top of the test section. The streamlines visualized by smoke sheets have been, then, captured by means of a compact camera.

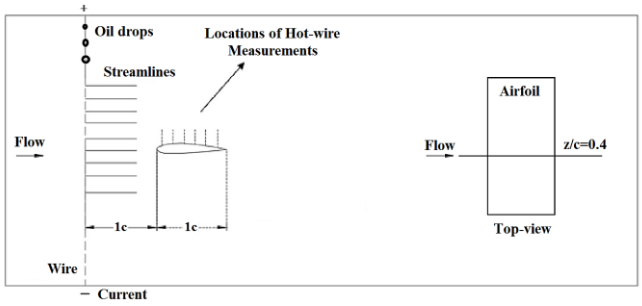

Fig. 2. A sketch of smoke-wire and hot-wire experiments

2.2 Velocity Distribution and Turbulence Statistics

Dual sensor probe has been utilized to obtain velocity distribution and U_{rms} values over suction surface airfoil. After calibration process, hot-wire probe has been positioned and run by means of traverse system and velocity measurements have been performed by starting from x/c=0.1 to x/c=1.0 (x refers to the distance of leading-edge) with 0.1c intervals. During the experiment, 2 kHz has been selected as the sample rate and 20480 data has been collected.

Regarding equations, averages of u velocity component and the velocity standard deviation have been calculated with Equation (1), Equation (2), respectively as follows:

$$U_{mean} = \frac{1}{N}\sum_{i}^{N} U_i \quad (1)$$

$$U_{rms} = \left(\frac{1}{N-1}\sum_{i}^{N}\left(U_i - U_{mean}\right)^2\right)^{0.5} \quad (2)$$

2.3 Shear Stress Measurement

As the researchers found in their study [5, 16, 17], the exploration boundary layer separation, transition and LSB phenomena based on wall shear stress measurement via hot-film sensors have been performed in this letter. Since the total heat transfer from the hot-film sensor may be negatively affected because of undesired factors such as model material and flow properties [18], the calibration process of the hot-film sensor is too complicated. Therefore, the quasi-wall shear stress measurement in this letter has been recognized as carried out by Zhang et al. in their study [19]. They identified:

$$\tau = \left(\frac{E^2 - E_0^2}{E_0^2}\right)^3 \quad (3)$$

where E means output voltage while E_0 indicates the air temperature's voltage with no flow condition in the test section. During the experiment, data has been recorded via multi-channel Constant Temperature Anemometer (CTA) at the line of z/c=0.4 and along the chordwise from x/c=0.1 to x/c=0.8.

3 Results

3.1 Smoke-wire results

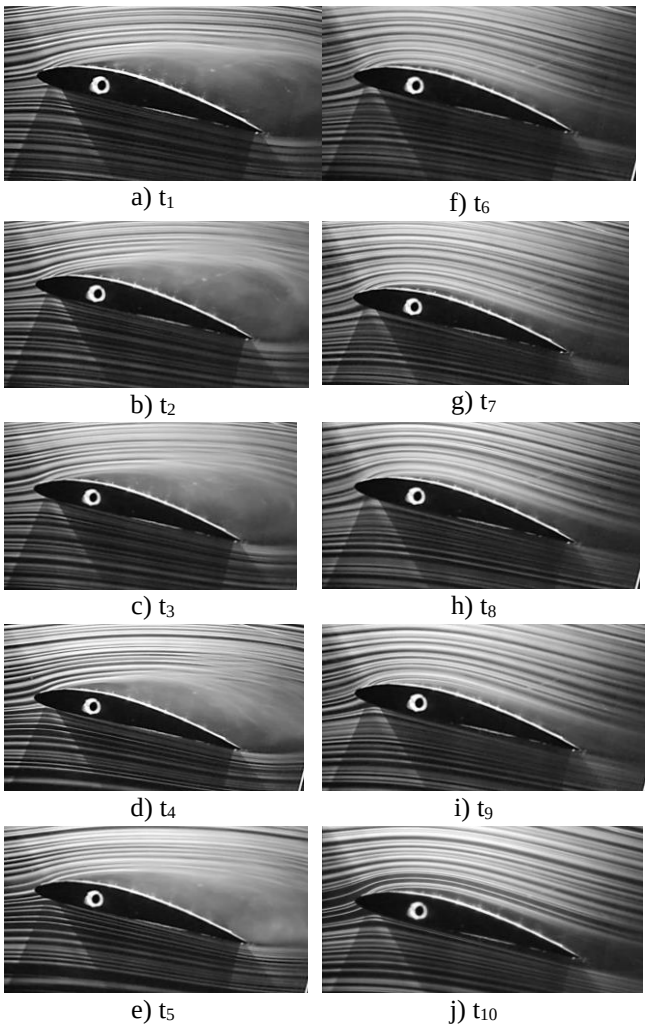

Fig. 3. Results of time-dependent smoke-wire experiment $Re=5x10^4$, $\alpha=14^o$.

From the results of time-dependent smoke-wire experiments at $Re=5x10^4$, $\alpha=14°$ in Figure 3, two different flow phenomena have observed over the airfoil owing to unsteady flow at low Reynolds number. In the experiment, duration t_1-t_5, it has been observed that flow separation has occurred at the distance of 15% chord length from the leading edge (x/c=0.15), due to the fact that long bubble burst as a result of the presence of favourable role APG (dP/dx>0). During t_1-t_3 (Figure 3(a)-(c)) the leading-edge separation between x/c=0.15 and x/c=0.70, located between x/c=0.15 and x/c=0.35 at t_4 and t_5 (Figure 3(d)-(e)). This means the shorten bubble, which leading edge vortex becomes small (inherently have bigger frequencies). It causes more vibrations and noise especially at trailing edge of airfoil (another trace of unsteadiness). On the other hand, the condition at which reattachment to the surface occurs has been observed in conjunction with the image sequences indicated from Figure 3(f) to Figure 3(j). Unlike in Figure 3(a)-3(e), APG could not play a dominant role on flow, result in emerging the condition, at which boundary layer separation does not form even though they have been performed with same Reynolds number and angle of attack. As seen the authors' previous study [5], LSB forming at leading-edge of the airfoil especially at α=10° and α=12° might burst based on Reynolds number, resulting in leading-edge separation and abrupt stall. Figure 3 shows the unsteady leading-edge separation based on the interaction of APG and laminar flow.

3.2 Velocity Distribution and U_{rms} Results

u/U velocity profile over the airfoil obtained from hot-wire measurement results have been illustrated as seen in Figure 4. In this figure, the boundary layer (dashed line) and separations (solid line) were sketched based on velocity profile over the airfoil. It is clearly shown that the flow at x/c=0 and x/c=0.1 is laminar. As observed at results of the smoke-wire experiment where flow separation has occurred, the velocity at x/c=0.2 has abruptly decreased in the boundary layer, indicating that flow has started to separate from the solid surface because of APG. Moreover, it has been noticed that larger vortices trajectory has occurred near the boundary layer. These statements have caused the flow, which has different frequencies (a trace of unsteadiness), to occur to the surface of the airfoil. Furthermore, moving downstream the velocity fluctuations owing to the boundary layer instability have been amplified. These fluctuations having large momentum cause the unstable flow in the boundary layer to be had. Regarding the more detailed information of different physical mechanisms as observed at a study performed by Deng et al. [20], it has been revealed that surface (or leading-edge vortex) vortex (SV) between at x/c=0.6 and x/c=0.8 occurs near the boundary layer. After x/c=0.8, larger vortex called as trailing-edge vortex (TEV) having more momentum are formed due to the wake effects. These two flow characteristics near the boundary layer cause

the alternating downstream shedding to occur, resulting in different periodic characteristics in the wake flow [5].

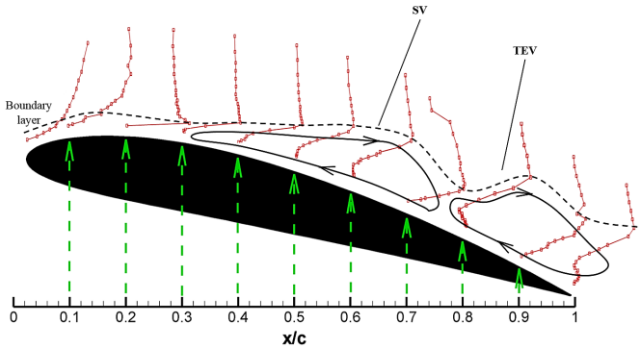

Fig. 4. u/U velocity profile in the boundary layer of NACA 4412 airfoil.

Figure 5 shows the U_{rms} velocity profile, turbulent kinetic energy contours, separations (solid), the boundary layer (dashed) and maximum RMS (dash-dotted) lines sketched by authors based on velocity measurements over the airfoil. By comparison with Figure 4, the flow is laminar before x/c=0.2. After x/c=0.2, leading-edge flow separation has occurred. The maximum RMS line corresponds to the middle part of the SV and TEV separations. At the same time, it has been also pointed out that the highest values of maximum RMS line correspond with core region of the turbulent kinetic energy contour. Besides, the fluctuations in the flow have simultaneously increased along the downstream, promoting complex and chaotic flow behaviour at the trailing edge mostly due to the fact that the flow separations over the suction surface of the airfoil encounter with those coming from pressure surface. This situation is understood from zigzags in U_{rms} profile near the trailing edge.

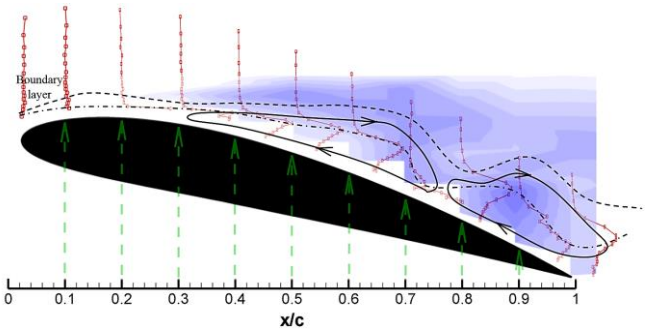

Fig. 5. U_{rms} profile and turbulent kinetic energy contours over the NACA 4412 airfoil.

3.3 Shear Layer Measurement Result

The different pathway of understanding of the physical characteristic of flow by performing the definite near-surface flow measurements has been shown with the results of hot-film sensors as denoted in Figure 6. y-axis at graphs illustrates the time-dependent voltage variance, whilst x-axis indicates the time (data has been recorded at 10 seconds during the hot-film experiment). As the flow is under the laminar regime before at x/c=0.2, therefore the voltage fluctuation is low. At x/c=0.2, surges in the voltages have started to increase, indicating the occurrence of boundary layer flow separation. Moreover, fluctuations in the voltage variances have apparently increased the downstream and have reached the peak levels especially x/c=0.6, x/c=0.7 and x/c=0.8. These means that more energized SVs and TEVs have been occurred at the trailing edge. Moreover; voltage undulations changes based on the time and occasionally the voltage peak occurs intermittently, which points out unsteady flow characteristic over the airfoil at the stall angle.

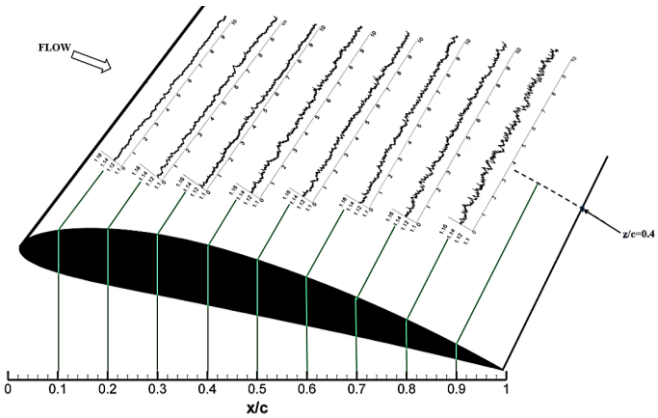

Fig. 6. Time-dependent voltage variance results of hot-film sensor.

4 Conclusion

As a conclusion, the experimental results have proven that the flow condition under low Reynolds number exhibits different regime over the surface of NACA 4412 airfoil: (*i*) boundary layer separation without reattachment due to the long bubble bursting, (*ii*) attached flow with a bubble. Besides, the frequency bands of fluctuations under the flow separation have exponentially amplified along downstream of airfoil and they have reached the top level probably with saturation of energized flow, resulting in emerging of unsteady and chaotic flow characteristics. Experimental results have also revealed that they exhibit a subordinate role with each other. Unsteady flow condition over the surface of the airfoil has inevitably emerged with these two flow phenomena, affecting flow regimes or aerodynamic performances of flight vehicles operating at low Reynolds number negatively.

References

1. B. H. Carmichael, NASA CR. (1981).
2. T. J. Mueller, J. D. DeLaurier, Annu. Rev. Fluid Mech. 35, 89-111, (2003)
3. E. J. Fitzgerald, T. J. Mueller. AIAA J, **28(4)**, 584-592, (1990).
4. M. O'meara, T. J. Mueller. AIAA J, **25(8)**, 1033-1041, (1987).
5. K. Koca, M. S. Genç, H. H. Açıkel, M. Çağdaş, T. M. Bodur. Energy, **144**, 750-764, (2018).
6. M. S. Genç, İ. Karasu, H. H. Açıkel. Exp. Therm. Fluid Sci., **39**, 252-264, (2012).
7. K. Koca, M.S. Genç, H.H. Açıkel. Çukurova Üniversitesi Mühendislik-Mimarlık Fakültesi Dergisi, **31(ÖS2)**, 127-134 (2016)
8. I. Rodríguez, O. Lehmkuhl, R. Borrell, A. Oliva, Int. J. Heat Fluid Flow, **43**, 194-203, (2013).
1. D. Simoni, M. Ubaldi, P. Zunino, D. Lengani, F. Bertini. Flow Turbul. Combust. **88**, 45-62, (2012).
9. L. E. Jones, R. D. Sandberg, N. D. Sandham. J. Fluid Mech., **602**, 175-207, (2008).
10. M. S. Genç, K. Koca, H. H. Açıkel, G. Özkan, M. S. Kırış, R. Yıldız. In EPJ Web Conf., **114**, 2029, (2016).
11. M.S. Genç, G. Özkan, M. Özden, M.S. Kırış, R. Yıldız. Proc IMechE, Part C: Journal of Mechanical Engineering Science, **232(22)**, 4019-4037 (2018)
12. I. Karasu, M. Özden, M.S. Genç, Journal of Fluids Engineering-Transactions of The ASME, 140(12) 121102-1-121102-15 (2018).
13. A. Ducoin, J. C. Loiseau, J. C. Robinet. Eur. J. Mech: B/Fluids, **57**, 231-248, (2016).
14. A. Lambert, S. Yarusevych. Phys. Fluids, 31(6), 064105, (2019).
15. M. S. Genç, K. Koca, H. H. Açıkel. Energy, **176**, 320-334, (2019).
16. H. H. Açıkel, M. S. Genç. Energy, **165**, 176-190, (2018).
17. C. Ghouila-Houri, J. Claudel, J. C. Gerbedoen, Q. Gallas, E. Garnier, A. Merlen, R. Viard, A.
18. Talbi, P. Pernod. Appl. Phys. Lett., **109(24)**, 241905, (2016).
19. H. H. Bruun. Meas. Sci. Technol.,7, 10, (1996).
20. X. Zhang, A. Mahallati, S. Sjolander. AIAA Conf., 3643, (2002).
21. J. Deng, L. Sun, X. Shao. Phys. Fluids, 31(2), (2019).